Vibration Suppression Performance of Piezoceramic and Magnetostrictive Materials in Hybrid Constrained Layer Damping

ARTICLE *in* PROC SPIE · JUNE 1999

DOI: 10.1117/12.349787

3 AUTHORS, INCLUDING:

Bishakh Bhattacharya
Indian Institute of Technology Kanpur
62 PUBLICATIONS **150** CITATIONS

Vibration Suppression Performance of Piezoceramic and Magnetostrictive Materials in Constrained Layer Damping

B. Bhattacharya*, J.A. Rongong and G.R. Tomlinson
Department of Mechanical Engineering, University of Sheffield, Sheffield, S1 3JD, UK.

ABSTRACT

Active constrained layer damping has been shown to be an effective way of controlling structural vibration. The success of the technique depends significantly on the strain imparted to the constraining layer by an actuator made of a smart material – typically a piezoelectric ceramic. The possibility of using magnetostrictive smart patches as actuators is explored in this regard. Comparisons of performance are made between commonly used piezoelectric ceramic and proposed magnetostrictive actuators on the basis of maximum power consumption. It is shown that magnetostrictives offer benefits particularly in the lower frequencies.

Keywords: Semi active vibration control, piezoceramic, magnetostrictive, constrained layer damping, viscoelastic damping

1. INTRODUCTION

Vibration suppression using constrained layer damping (CLD) is based on the dissipation of energy in a viscoelastic layer undergoing deformations caused by relative motion between the constraining layer and the host structure. The effectiveness of such an approach depends largely on the amount of shear induced in the viscoelastic material (VEM). Smart actuators such as patches of piezoelectric materials, have been used to enhance the induced shear in the VEM[1] by modifying the deformation of the constraining layer. Also, as the active elements are not positioned on the neutral axis of the beam, they can generate significant bending moments. The interaction of these effects in active constrained layer damping (ACLD) has been studied by many in the last decade[2-6] as the concept combines the stability of passive damping with the adaptability of smart actuation. In the work reported to date actuators have been made from piezoelectric (PZT or PVDF) materials that either replace or are bonded to the constraining layer. Other materials however, can also be used to induce strains – the ability of magnetostrictive materials such as Terfenol-D to generate large strains is well known. As magnetostrictives can be formed into composites of required shape and size using metallic or non-metallic binders[7], an investigation into their suitability as actuators for ACLD is of interest.

In this paper numerical simulations are made to investigate the effectiveness of magnetostrictive materials as the active elements in ACLD in comparison with PZT. Analyses are based on the Rayleigh-Ritz assumed series models developed by Rongong *et al*[6] for cantilever beams with ACLD. The effect of piezoelectrically driven ACLD on the dynamic response of a cantilever beam is first discussed in section 2. The use of a magnetostrictive induced strain actuator is considered in section 3. Finally, in section 4, a comparison of performance of piezoelectric and magnetostrictive material is made using the actuator power factor described by Liang *et al*[8].

2. EFFECT OF ACLD ON THE DYNAMIC RESPONSE OF A CANTILEVER BEAM

2.1 Theoretical Modelling

The variant of the ACLD concept considered here is shown in Figure 1 – a PZT actuator is bonded to a metallic constraining layer.

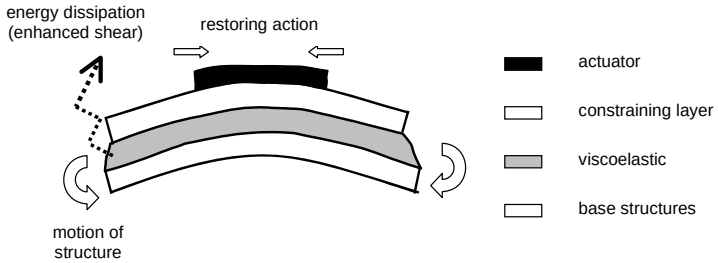

Figure 1: Concept of active constrained layer damping

*Correspondence: email:B.Bhat@sheffield.ac.uk; WWW:http://www.shef.ac.uk/--;Telephone:0044-114-22-27765 Fax: 0044-114-22-27890

Active strains are generated in the constraining layer by applying voltage across the PZT. The derivation of an analytical model for this configuration using Rayleigh-Ritz assumed series technique is outlined briefly here – a detailed discussion is given by Rongong *et al*[6].

The basic structure considered is cantilever beam with a symmetrical covering of CLD on either face as shown in Figure 2. PZT patches are applied symmetrically to either side on top of the constraining layer.

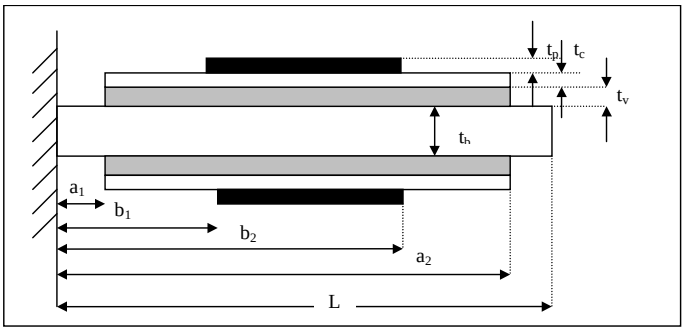

Figure 2: Cantilever beam model

Flexural deformations can be initiated by applying signals of opposite polarity to the PZTs on either side of the beam. Neglecting the flexural stiffness of the viscoelastic, PZT and constraining layers about their mid-surface the flexural motion is approximated by,

$$u_c(x,t) = \sum_{j=1}^{N_c} c_j(t) \cdot \psi_j(x) = \boldsymbol{\psi}^{\mathrm{T}}\mathbf{c} \tag{1}$$

$$w(x,t) = \sum_{j=1}^{N_w} b_j(t) \cdot \varphi_j(x) = \boldsymbol{\varphi}^{\mathrm{T}}\mathbf{b} \tag{2}$$

where, **c**, **b** are vectors of unknown time varying coefficients and $\boldsymbol{\psi}$ and $\boldsymbol{\varphi}$ are assumed shape functions corresponding to the longitudinal and transverse vibration of beam. For a cantilevered beam, these are given by:

$$\psi_j = \sin\frac{(2j-1)\pi}{2L}x; \quad j=1,2,3\ldots$$

$$\varphi_j(x) = \alpha_1 \sin(\frac{\lambda_j}{L}x) + \alpha_2 \cos(\frac{\lambda_j}{L}x) + \alpha_3 \sinh(\frac{\lambda_j}{L}x) +_1 \alpha_4 \cosh(\frac{\lambda_j}{L}x)$$

The constants λ and α are tabulated in books e.g. Blevins[9].

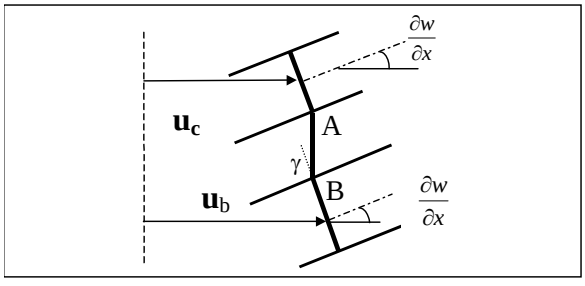

Figure 3: Shear angle of the viscoelastic layer in flexural motion

The shear angle of the viscoelastic layer as shown in Figure 3, is given by

$$\gamma = \frac{\partial w}{\partial x} + \frac{u_A - u_B}{t_v}, \qquad u_A = u_c + \frac{t_c + t_p}{2} \cdot \frac{\partial w}{\partial x} \text{ and } \quad u_B = u_b + \frac{t_b}{2} \cdot \frac{\partial w}{\partial x} \tag{3}$$

The subscripts *p, c, v, b* stands for the PZT, constrained layer, viscoelastic layer and the host beam respectively. For, one dimensional application, the piezoelectric equation may be written as –

$$\varepsilon_l = \frac{\sigma_p}{E} + \frac{d_{31}}{t_p} V \tag{4}$$

where, ε_l denotes the strain generated by the piezoelectric in the longitudinal direction, σ_p denotes the stress in the piezoelectric actuator, d_{31} the piezoelectric constant, t_p the thickness of the actuator and V the applied voltage.

The kinetic energy expression is given by,

$$T = [T_b + 2\{T_v + T_c + T_p\}]_{flexural} + [2\{T_v + T_c + T_p\}]_{long}$$

where,

$$T_{flexural_{total}} = \frac{1}{2}\int_0^L m_b \dot{w}^2 \, dx + 2\{\frac{1}{2}\int_{a1}^{a2} (m_v + m_c)\, \dot{w}^2 dx + \frac{1}{2}\int_{b1}^{b2} m_p \dot{w}^2 dx\} \tag{5}$$

$$T_{long_{total}} = 2\{\frac{1}{2}\int_{a1}^{a2} m_v \frac{4\dot{u}_c{}^2 + 2\dot{u}_c \dot{w}'^2 t_b^2}{12} dx + \frac{1}{2}\int_{a1}^{a2} m_c \dot{u}_c^2 \, dx + \frac{1}{2}\int_{b1}^{b2} m_p \dot{u}_p^2 \, dx\} \tag{6}$$

The strain energy expression is given by,

$$U = U_b + 2\{U_v + U_c + U_p\} \tag{7}$$

$$U_b = \frac{1}{2}\int_0^L E_b I_b (w'')^2 dx, U_v = \frac{1}{2}\int_{a1}^{a2} A_v G_v (\frac{u_c + w' \frac{t_d}{2}}{t_v})^2 dx, U_c = \frac{1}{2}\int_{a1}^{a2} A_c E_c (u_c')^2 dx, U_p = \frac{1}{2}\int_{b1}^{b2} A_p E_p (u_c'^2 - 2u_c' \mu V + \mu^2 V^2) dx$$

where, *E, G, I* and *A* denote the Young's modulus, shear modulus, moment of inertia and the cross-sectional area of the corresponding layers of beam respectively. Substituting the energy expressions into the Lagrange's equation and including the hysteric damping the steady state equation of motion may be written as

$$[M]\ddot{q} + [C]\dot{q} + [K]q = PV + F \tag{8}$$

where, M, *C* and *K* are the mass, damping and stiffness matrices, *F* denotes the force vector, *q* the DOF, *P* the force-voltage coupling vector and *V* the applied voltage in PZT.

2.2 Numerical Simulation using PZT actuators

The effect of ACLD is demonstrated by considering the behaviour of an aluminium cantilever beam with CLD layers on either side. The viscoelastic material used is ISD 112 (manufactured by 3M) and the constraining layers are also of aluminium. PZT patches are fixed over the constraining layer at a location where they can impart maximum strain to the structure. The geometric and material properties are given in Table 1.

Component	**Material**	**Coverage (mm)**	**Cross Section (mm × mm)**	**Elastic mod. (MPa)**	**Loss Factor**	**Density (kg/m^3)**	**d_{31} ($\times 10^{-12}$)**
Beam	Aluminium	0-153	38 × 3.175	70,000	0.004	2700	0
Viscoelastic	ISD112	0-153	38 × 0.127	0.1-10	0.5-1.1	1600	0
Cons. layer	Aluminium	0-153	38 × 0.254	70,000	0.004	2700	0
PZT actuator	Sonox P5	23-53	30 × 0.400	62,500 (E_{11})	0.011	7700	-180

Table 1: Dimensions and material properties of simulated beam with ACLD

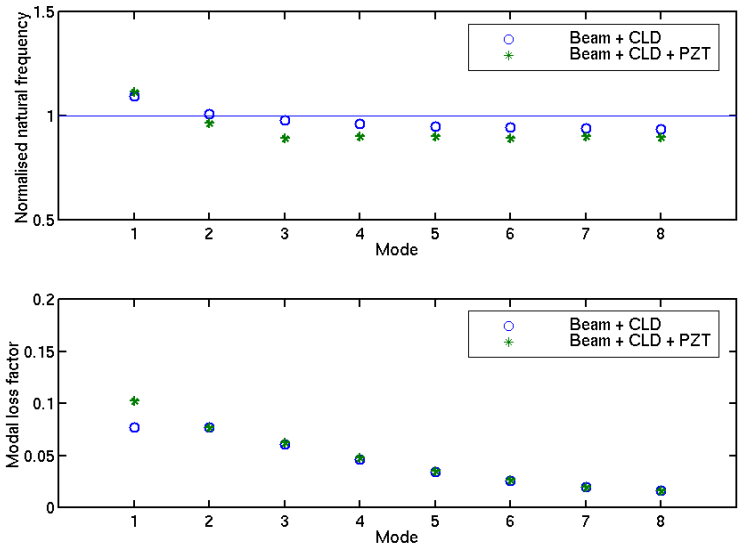

Figure 4: Normalised natural frequencies and passive models loss factors for various damping configurations

Figure 4 shows the effect of adding CLD and PZT layers on the natural frequencies and modal loss factors. The natural frequencies are presented as a fraction of the natural frequency of the plain beam. It can be seen that the added layers increase the frequency in the low modes but reduce it in the high ones. It can also be seen that that the loss factors are near optimal for the first two modes but then decrease in the higher modes. For passive damping the added stiffness of the PZT only significantly affects the first mode. In Figure 5 the steady state frequency response is plotted for the beam with a unit load at its free-end. In this case the actuators are driven with a control voltage proportional to the beam-tip velocity. Notice that although the first mode resonance is reduced by the active action the third mode level is increased due to non-collocation.

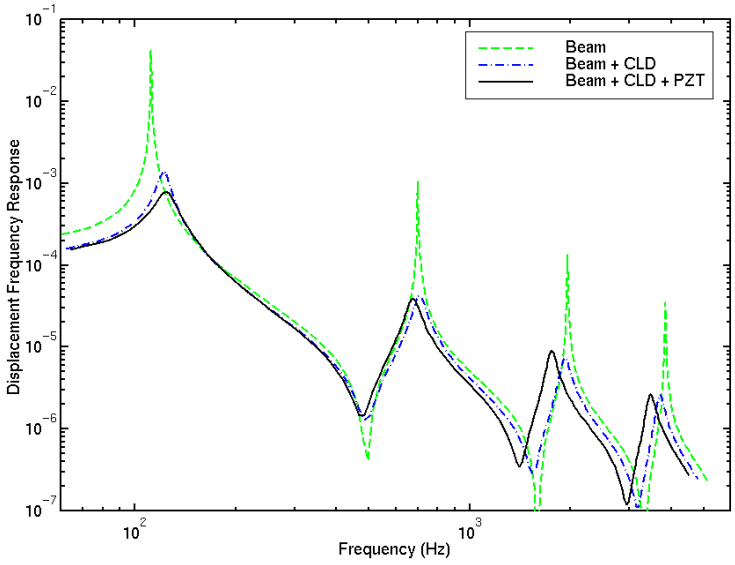

Figure 5: Change in steady state response for various damping configurations

3. ACLD USING MAGNETOSTRICTIVE ACTUATORS

In order to investigate the performance of a magnetostrictive actuator in ACLD the model described in the previous section must be modified. The expression for induced strain becomes,

$$\varepsilon_l = \frac{\sigma_m}{E} + d_m H \tag{9}$$

where d_m denotes the magnetomechanical constant and H the magnetic field intensity. If the magnetic field is generated by passing a current of magnitude I through coils with N turns around the actuator, H may be obtained from,

$$H = \frac{N}{\sqrt{r_a^{\,2} + l_a^2}} I \approx \frac{N}{l_a} I \qquad \text{as} \quad l_a >> r_a \tag{10}$$

where, r_a and l_a are the effective coil radius and the length of the actuator respectively.

The performance of ACLD with magnetostrictive actuators is considered using two different host beams, isotropic aluminium and composite laminate (Case A and B respectively. As in the previous section, both sides of the host beam are covered by the viscoelastic and constraining layers and two magnetostrictive actuators are attached on top. The geometric and material properties are given in Table 2.

Component	Material	Coverage (mm)	Cross Section (mm × mm)	Elastic mod. (MPa)	Loss Factor	Density (kg/m^3)	d_m ($\times 10^{-9}$)
Beam (case A)	Aluminium	0-153	38 × 3.175	70,000	0.004	2700	0
Beam (case B)	GRP	0-153	38 × 3.175	20,700	0.005	1600	0
Viscoelastic	ISD112	0-153	38 × 0.127	0.1-10	0.5-1.1	1000	0
Cons. layer	Aluminium	0-153	38 × 0.254	70,000	0.004	2700	0
MS actuator	Terfenol-D	23-53	30 × 0.400	17,700 (E_{11})	0.018	6800	5.9

Table 2: Dimensions and material properties of simulated beams with magnetostrictive ACLD

3.1 Performance of magnetostrictive actuators with ACLD on an aluminium beam

The effect on the passive properties of beam type A can be seen in Figure 6.

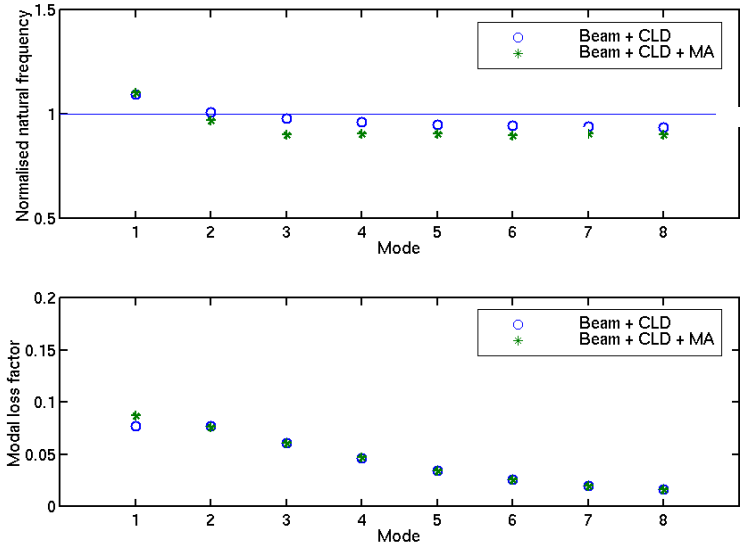

Figure 6: Normalised natural frequencies and passive modal loss factors for beam A

Apart from the first mode the frequencies are reduced by the addition of the ACLD layers. The increase in passive damping of the first mode by adding the actuators is less noticeable than with PZT (compare Figures 4 & 6) as the Terfenol-D actuators are much more flexible. Figure 7, shows the change in steady state frequency response of the beam with unit load at its free end is shown. Assuming a magnetic filed generated by a coil with 5 turns/mm a gain of 100 is applied to the feedback current. The effect of damping is clearly visible in the first four modes. Note again the effect of non-collocation for mode 3.

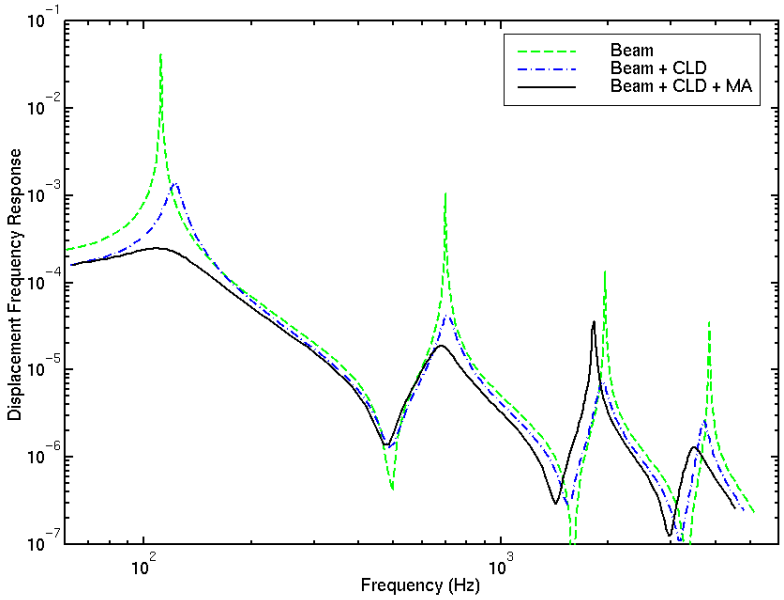

Figure 7: Change in steady state response for beam A

3.2 Performance of magnetostrictive actuators with ACLD on a composite beam

The performance of ACLD employed with a composite host beam (rather than an isotropic aluminium one) is presented in Figures 8 and 9. In Figure 8 it can be seen that significant increases in natural frequency occur in the low modes through the addition of the ACLD layers as the host beam is much more flexible. The increase in modal loss factors is also significant. Figure 9 shows that active actuation is highly effective – whether in improving or degrading the performance of the passive case. The simulation shows that magnetostrictive actuators could be used more successfully to reduce structural vibration in structures with lower modulus of elasticity.

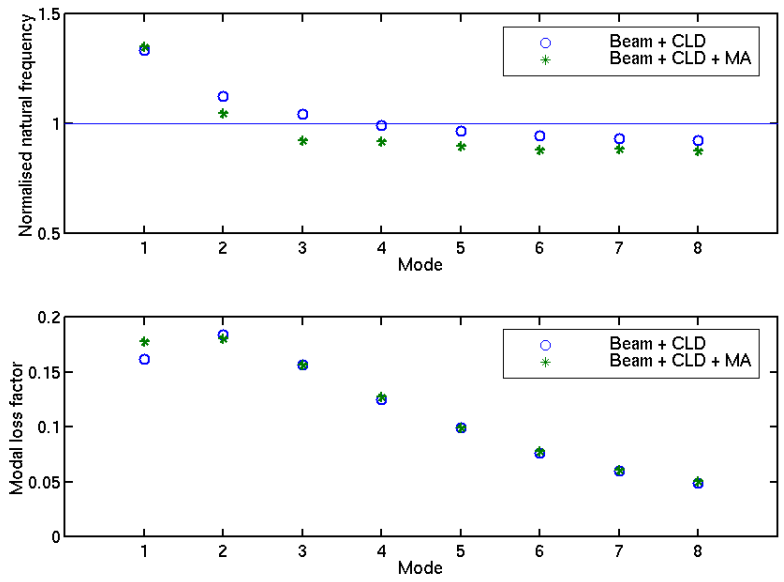

Figure 8: Normalised natural frequencies and passive modal loss factors for beam B

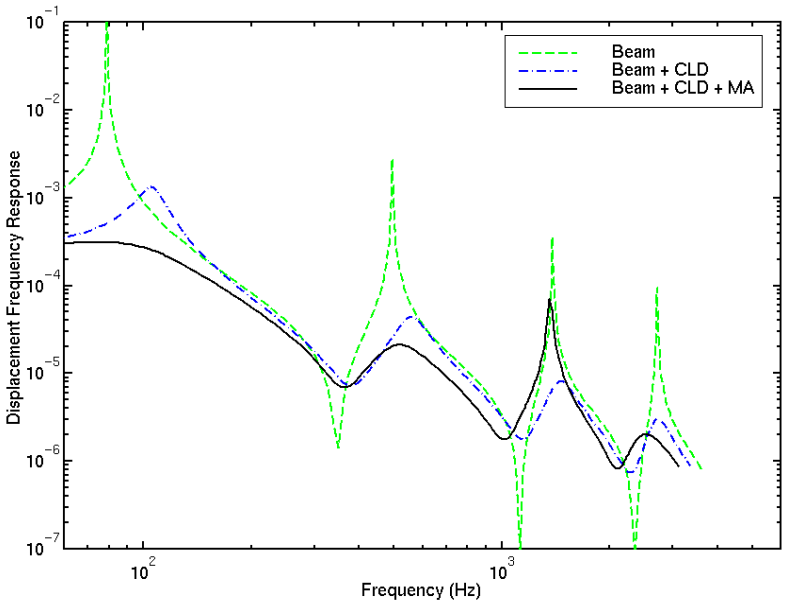

Figure 9: Change in steady state response for beam B

In composite laminate the ply lay-up plays significant role in the dynamical behaviour of the beam. In a comparative study 3 GRP laminates with ply sequence 0_8, 90_8 and $[\pm 45]_4$ respectively are chosen. Figure 10 shows the steady state response to a unit load at the free end of the beam corresponding to these cases. It is observed that for first mode, although the frequency has come down from 220 Hz at 0_8 ply sequence to 115 Hz at 90_8 ply sequence, the damping has increased considerably from 5.6% at 0_8 ply sequence to 6.7% at $[\pm 45]_4$ ply sequence and to a very high 13.89% at 90_8 ply sequence. This also shows that the magnetostrictive actuator works better with the softer laminate.

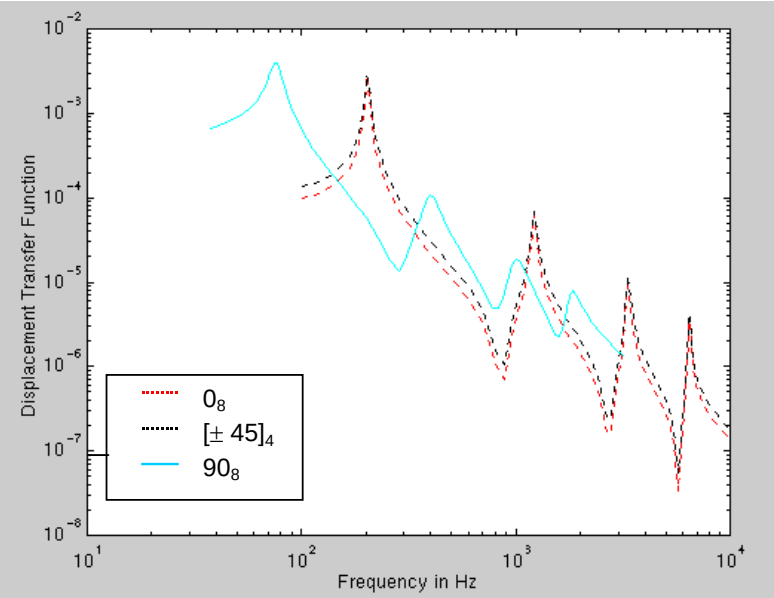

Figure 10: Frequency response of beams with different ply lay-up + ACLD with magnetostrictive actuators

4. A COMPARISON IN PERFORMANCE BETWEEN PZT AND MAGNETOSTRICTIVE ACTUATOR

PZT actuators are activated by applying a considerable voltage across them, while in case of magnetostrictive actuators, the excitation is carried out by applying current in the coils around the patch. This difference in input makes it difficult to compare their performance directly. However, in such cases, the actuator power factor corresponding to the two types of actuators could be computed following the procedure suggested by Liang *et al*[5]. Following this procedure, the energy efficiency of the actuator, which is also the ratio of dissipative mechanical power to the supplied electric power in driving the structure, is defined as:

$$\psi = \frac{\mathrm{Re}(Y_s)}{|Y_s|} \tag{11}$$

where Y_s is the admittance of the coupled electro-mechanical system. For a frequency range of excitation much below the resonating frequency of the actuator, the admittance Y_s may be expressed as:

$$Y_s = iw\frac{w_A l_A}{h_A}(\varepsilon_{33}^{-t} - \frac{Z_s}{Z_s + Z_A} d_{32}^2 Y_{22}^{-E}) \tag{12}$$

Where w_A, lA and h_A are the width, length and thickness of the actuator respectively, Z_s and Z_A the impedance of the structure and the actuator respectively, d_{32} the piezoelectric constant, Y_{22}^{E} the complex elastic modulus of the actuator and ε_{33} the complex dielectric constant. A similar expression can be derived for the magnetostrictive material changing the complex dielectric constant by the complex permittivity of the material. On the basis of this factor, a similar cantilever beam as defined in Section 3 (Case B) is chosen to compare the efficiency of the two types of materials. Material properties of the actuators are chosen according to Table 1 and 2. The results are shown in Figure 13. It is interesting to note that the actuator power factor is significantly higher for magnetostrictive actuators in the lower modes. However, at higher modes, PZT gives better performance in terms of actuator power factor. The highest actuator power factor obtained for magnetostrictive material is about 89% for the second mode, while for PZT it is about 81% for the eighth mode. The cause of the increase in performance of PZT may be due to their higher modulus of elasticity resulting in better impedance matching in the higher modes.

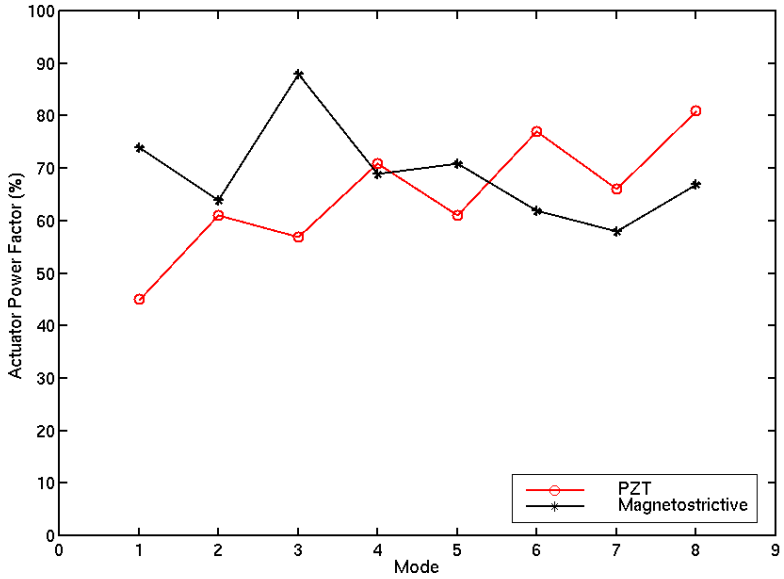

Figure 11: Actuator power factor with ACLD on beam B

5. CONCLUSIONS

The concept of active constrained layer damping has been briefly illustrated with numerical simulations of the dynamical behaviour of a cantilevered beam. Such simulations are extended to allow the use of a magnetostrictive actuator.

It has been shown that the actuators made of magnetostrictive materials could be used successfully in active constrained layer damping. The performance of the actuator with beams made of different materials and ply lay-ups are evaluated. In all the cases the addition of magnetostrictive actuator has resulted in improved damping performance. A comparison between the performance of PZT and magnetostrictive actuators carried out on the basis of actuator power factor has shown that the a magnetostrictive actuator is best for the low modes of vibration while for higher modes PZT shows better performance.

REFERENCES

1. Plump J M and Hubbard J E, "Modelling of an active constrained layer damper", 12th International Congress on Acoustics, Paper D41, Toronto, July 1996.

2. Baz A and Ro J, "The concept and performance of active constrained layer damping", *Journal of Sound and Vibration*, 28, 18-21, 1994.

3. Liao W H and Wang K W, "A new active constrained layer configuration with enhanced boundary actions", *Smart Materials and Structures*, 5, 638-648, 1996.

4. Shen I Y, "Hybrid damping through active constrained layer treatments", *ASME Journal of Vibration and Acoustics*, 116, 341-349, 1994.

5. Van Nostrand W C, Knowles G J and Inman D J, "Active constrained layer damping for micro-satellites", *Dynamics and Control of Structures in Space*, II, 667-681.

6. Rongong J A, Wright J R, Wynne R J and Tomlinson G R, "Modelling of a hybrid constrained layer/piezoceramic approach to active damping", *ASME Journal of Vibration and Acoustics*, 119, 120-130, January 1997.

7. Sandlund L, Fahlander M, Cedell T, Restorff J and Clark A E, "Magnetostriction, elastic moduli and coupling factors of composite Terfenol-D", *Journal of Applied Physics*, 75 (10), 5656-5658, 1994.

8. Liang C, Sun F P and Rogers C A, "Design of optimal actuator location and configuration based on actuator power factor", Proceedings of the Fourth International Conference on Adaptive Structures, Cologne, Germany, 2-4 Nov 1993.

9. Blevins R D, *Formulas for natural frequency and mode shape*, Van Nostrand Reinhold, New York, 1979.